Fourier-transform infra-red and birefringence studies of orientation in uniaxially stretched poly(methyl methacrylate)–poly(trifluoroethylene) blends

Y. Zhao, B. Jasse* and L. Monnerie

Laboratoire de Physicochimie Structurale et Macromoléculaire, Ecole Supérieure de Physique et de Chimie, 10 rue Vauquelin, 75231 Paris Cedex 05, France

(Received 16 October 1989; revised 20 February 1990; accepted 22 February 1990)

Orientation of both polymer chains in compatible blends of poly(methyl methacrylate)–poly(trifluoroethylene) (PMMA–PF_3E) has been studied using Fourier-transform infra-red and birefringence measurements. Two different behaviours are observed depending whether or not PF_3E crystallizes. In the concentration range where the material remains homogeneous, i.e. up to 10% of PF_3E, one observes an increase of PMMA orientation with respect to the pure polymer, at the same drawing temperature $T - T_g$. In this domain, PF_3E orientation is insensitive to the concentration of this polymer in the blend. When PF_3E crystallizes, a small amount of PF_3E ($\sim 3\%$) remains in the PMMA amorphous phase. Thus, the orientation of PMMA is insensitive to the original PF_3E concentration and remains higher than the orientation observed in pure PMMA under the same experimental conditions ($T - T_g = \text{constant}$). The orientation of the semicrystalline PF_3E phase increases with crystallinity but remains insensitive to the stretching temperature. The orientation behaviour is well explained by a change of the friction coefficient and by the existence of a physical network originating from the presence of crystallites in crystallized blends.

(Keywords: poly(methyl methacrylate); poly(trifluoroethylene); polymer blends; orientation; Fourier-transform infra-red; birefringence)

INTRODUCTION

In a previous paper[1] we described the orientation behaviour of poly(methyl methacrylate) (PMMA)–poly(ethylene oxide) (PEO) blends subjected to uniaxial strain above the glass transition temperature. PMMA orientation is greater in the blends than in the pure polymer under the same experimental conditions of stretching (same $T - T_g$ and strain rate $\dot{\varepsilon}$), while PEO chains remained unoriented whatever the PEO molecular weight. The results were interpreted in terms of a hindrance to relaxation of PMMA chains induced by a modification of the friction coefficient that arose due to the molecular interactions caused by compatibility.

PMMA is also compatible with fluorinated polymers such as poly(vinylidene fluoride) (PVF_2) and poly(trifluoroethylene) (PF_3E) and it was interesting to extend the previous study to such blends. Unfortunately, PVF_2 is insoluble in many common solvents and we did not succeed in preparing films from dimethylacetamide or dimethylformamide solutions that were thin enough for infra-red examination and had sufficiently good mechanical properties for stretching. On the other hand, PF_3E is soluble in methyl acetate and the preparation of thin films of PMMA–PF_3E blends is easily feasible.

Compatibility of PMMA–fluorinated polymer blends

Compatibility of PMMA–PVF_2 blends has been ascertained in the literature by various methods for probing the structure of the blends over characteristic dimensions ranging from micrometres to ångströms[2–9]. Only one glass transition temperature is observed in these blends. PVF_2 is able to crystallize when the weight fraction of the polymer is more than 0.5[2,10]. The Flory–Huggins parameter in the blends was measured by the melting-point depression method and found to be $\chi_{12} = -0.295$ at 160°C[3].

As compared to PVF_2, the compatibility of PMMA–PF_3E blends has been the subject of few studies. PF_3E presents a great number of structural defects due to head-to-head and tail-to-tail addition of monomer units during free-radical polymerization[11,12]. Furthermore, this polymer is essentially atactic[13]. Nevertheless, PF_3E chains are able to crystallize and the structure and morphology of different samples were studied by Lovinger and Cais[14]. In an infra-red spectroscopic study of model molecules of PMMA blended with PF_3E, Léonard *et al.*[15] have shown that intermolecular interactions in such blends appear to be stronger than in PMMA–PVF_2 blends.

The present work deals with the study of orientation of PMMA–PF_3E blends using infra-red dichroism and birefringence measurements.

EXPERIMENTAL

The PMMA used was a pure polymer obtained by radical chain polymerization ($\bar{M}_n = 63\,200$; $\bar{M}_w = 108\,000$; $T_g = 122$°C; tacticity, triads (%), $rr = 55$, $rm = 39$, $mm = 6$). The two PF_3E samples were industrial products from Atochem. Viscosity measurements performed in methyl

* To whom correspondence should be addressed

0032-3861/91/0200209-06

acetate at 30°C gave $[\eta] = 1.0$ dl g^{-1} for sample $PF_3E/1$ and $[\eta] = 1.1$ dl g^{-1} for sample $PF_3E/2$.

Sample preparation

Thin films suitable for infra-red spectroscopy were obtained by casting a 6% methyl acetate solution on a glass plate. Subsequent annealing was done under vacuum for 30 h at 120°C in order to remove any trace of solvent and internal stress. The glass transition temperatures of the samples were obtained using a Du Pont 1090 differential scanning calorimeter at a heating rate of 20°C min^{-1}; sample weight was ~7 mg. As previously observed by Wang and Porter in oriented polystyrene[16], the glass transition temperature of PMMA and compatible blends is uninfluenced by drawing in the limit of experimental accuracy.

Oriented samples from thin films were obtained on an apparatus developed in our laboratory, i.e. a stretching machine operating at constant strain rate and a special oven to obtain a very good temperature stability over the whole sample (homogeneity is ~0.05°C). Draw ratios were measured using ink marks on the sample. All the measurements were normalized to T_g. As a matter of fact, in amorphous polymers or compatible blends, T_g is a characteristic temperature above which motions of chain segments occur and it seems reasonable to choose T_g as a reference temperature for chain mobility. This choice is supported experimentally by the results obtained in polystyrene ($T_g = 107$°C), poly(*o*-chlorostyrene) ($T_g = 134$°C) and their compatible blends, where similar levels of orientation are obtained in samples stretched at $T = T_g + 11.5$°C[17]. Other experimental details on infra-red dichroism and birefringence measurements may be found in ref. 1.

Crystallization of PF_3E in the blends

Similarly to PVF_2, PF_3E is able to crystallize in the blends containing more than 10% of the polymer. As shown in *Table 1* and *Figure 1*, only one glass transition is observed in the as-cast blends up to a concentration of 20% of $PF_3E/1$ and 10% of $PF_3E/2$. Such samples are transparent while above these concentrations a whitening is observed, indicating that PF_3E crystallization occurs. However, about 10% of PF_3E in PMMA–$PF_3E/1$, T_g values do not fit a regular curve and scattered values are observed, similar to the behaviour noted in PMMA–PVF_2 blends above a concentration of 25% of PVF_2 in PMMA[3], and assigned to crystallization of PVF_2. After annealing the previous samples for 20 min at 220°C, PF_3E crystallizes, as can be seen on the thermograms given in *Figure 1*. On the other hand, a thermal treatment at 140°C, which corresponds to the highest temperature used to stretch the samples, does not induce crystallization up to an amount of 10% of PF_3E. Thus, homogeneous blends can be studied in this concentration range. Stretching an as-cast sample containing 20% of $PF_3E/1$ at 124°C and a strain rate $\dot{\varepsilon} = 0.026$ s^{-1} induces crystallization under stress of this polymer as shown by the thermogram given in *Figure 2*.

Table 1 Glass transition temperatures (°C) for each blend

	PF_3E (%)			
Blend	5	10	15	20
PMMA–$PF_3E/1$	111	101	109	101
PMMA–$PF_3E/2$	113	103		

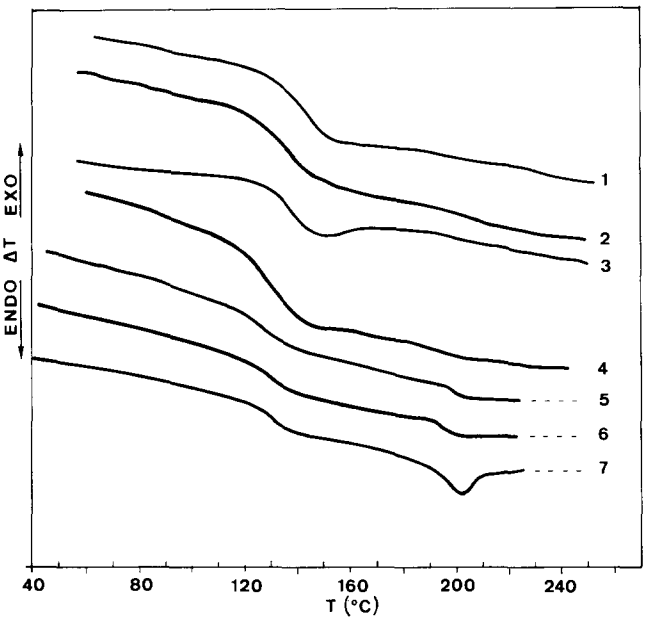

Figure 1 D.s.c. curves of PMMA–PF_3E blends. As-cast samples: (1) 5% PF_3E; (2) 10% PF_3E; (3) 15% PF_3E; (4) 20% PF_3E. Annealed samples (20 min; 220°C): (5) 5% PF_3E; (6) 10% PF_3E; (7) 20% PF_3E

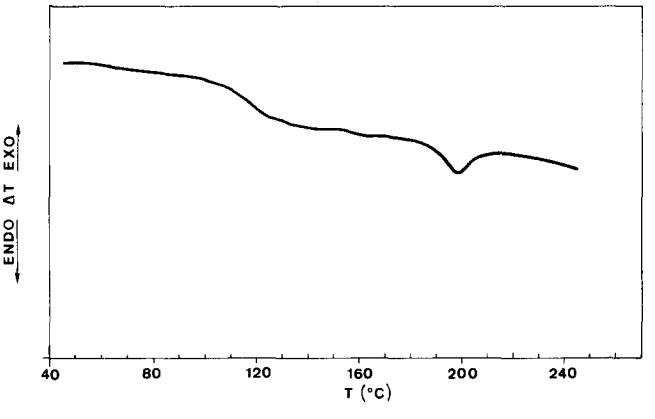

Figure 2 D.s.c. curve of a sample containing 20% PF_3E stretched at 124°C, $\dot{\varepsilon} = 0.026$ s^{-1} at a draw ratio $\lambda = 3$

RESULTS

Orientation measurements

For any absorption band, the dichroic ratio $R = A^{\parallel}/A^{\perp}$ ($A^{\parallel}$ and $A^{\perp}$ being the measured absorbance for electric vector parallel and perpendicular, respectively, to the stretching direction) is related to the second-order moment of the orientation function according to the relation:

$$\langle P_2(\cos\theta)\rangle = \frac{1}{2}(3\langle\cos^2\theta\rangle - 1) = \frac{R-1}{R+2}\frac{R_0+2}{R_0-1} \quad (1)$$

with $R_0 = 2\cot^2\alpha$, where α is the angle between the dipole moment vector of the considered vibration and the chain axis and θ is the angle between the local chain axis, defined as the axis joining two adjacent CH_2 groups in the main chain, and the draw direction[18].

Although infra-red spectroscopy is an attractive

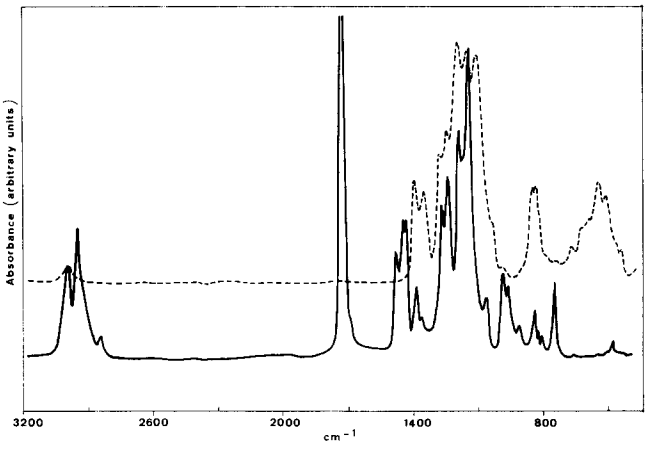

Figure 3 Infra-red spectra of PMMA (———) and PF_3E (---)

method of deducing the chain orientation of the different polymers in a blend, overlapping absorption bands may restrict the possibility of analysis. As shown in *Figure 3*, PMMA orientation can be measured using the 749 cm^{-1} absorption band, which is assigned to a skeletal vibrational motion affected by the CH_2 rocking vibration[19]. The α angle of the dipole moment vector of this vibration was measured at 17° (ref. 20). PF_3E orientation may be estimated using the 540 cm^{-1} absorption band, which can be tentatively assigned to a CF_2 group vibration according to the vibrational analysis of PVF_2[21].

Birefringence Δ in an oriented compatible blend is related to individual orientation functions[22] by the relation:

$$\Delta = f_1\Delta_1^0\langle P_2(\cos\theta)\rangle_1 + f_2\Delta_2^0\langle P_2(\cos\theta)\rangle_2 \qquad (2)$$

where f_i, Δ_i^0 and $\langle P_2(\cos\theta)\rangle_i$ are the volume fraction, intrinsic birefringence and orientation function of component i, respectively.

We shall consider successively orientation in homogeneous blends (up to an amount of 10% of PF_3E) and in blends where PF_3E has crystallized.

Orientation in homogeneous PMMA–PF_3E blends

PMMA orientation. All the samples were stretched at constant strain rate above the glass transition temperature. First consider the results obtained at a stretching temperature $T = T_g + 23°C$ and a strain rate $\dot{\varepsilon} = 0.026\ s^{-1}$ for different PMMA–PF_3E/1 blends. *Figure 4* illustrates the change of the $\langle P_2(\cos\theta)\rangle$ orientation function relative to PMMA as a function of draw ratio and PF_3E/1 percentage. Similarly *Figure 5* shows the change of PMMA orientation function as a function of draw ratio and PF_3E/2 percentage in blends stretched at a temperature $T = T_g + 17°C$ and $\dot{\varepsilon} = 0.026\ s^{-1}$. In both cases, introduction of PF_3E in PMMA induces a progressive increase of the orientation of PMMA chains.

PF_3E orientation. As far as PF_3E orientation is concerned, the absorption band at 540 cm^{-1} is not strong enough in the blends containing 5% of this polymer to allow measurements. The angle α of this vibration is unknown, so orientation of PF_3E/1 in the 10% blend stretched at $T = T_g + 23°C$ and $\dot{\varepsilon} = 0.026\ s^{-1}$ was characterized using the quantity $(R-1)/(R+2)_{540}$, which is proportional to $\langle P_2(\cos\theta)\rangle_{PF_3E}$. The results are given in *Figure 6*. A rectilinear relation holds between $(R-1)/(R+2)_{540}$ and draw ratio.

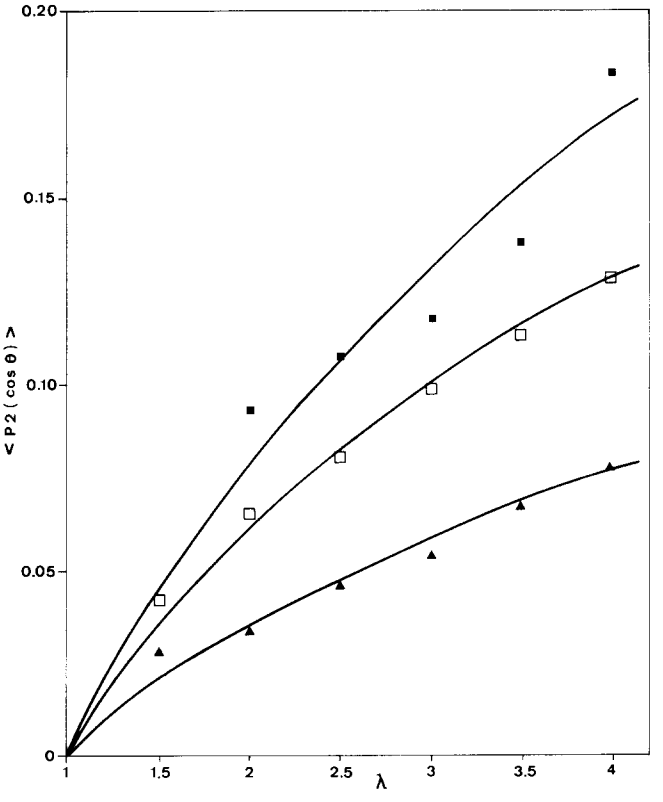

Figure 4 Orientation function of PMMA in PMMA–PF_3E/1 blends as a function of draw ratio. Temperature of stretching $T = T_g + 23°C$. Strain rate $\dot{\varepsilon} = 0.026\ s^{-1}$. Symbols: (▲) pure PMMA; (□) blend 5% PF_3E; (■) blend 10% PF_3E

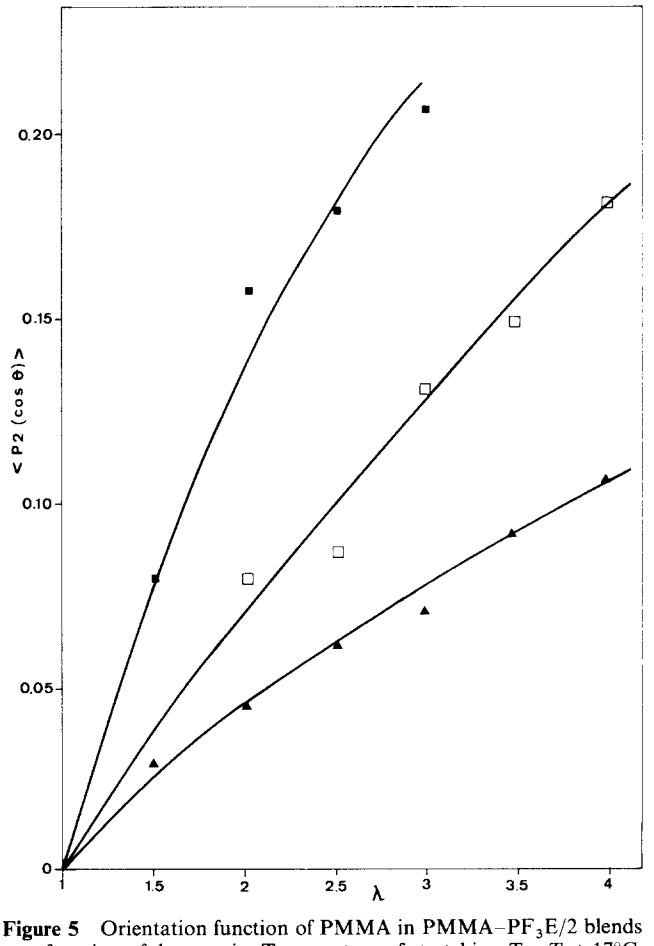

Figure 5 Orientation function of PMMA in PMMA–PF_3E/2 blends as a function of draw ratio. Temperature of stretching $T = T_g + 17°C$. Strain rate $\dot{\varepsilon} = 0.026\ s^{-1}$. Symbols: (▲) pure PMMA; (□) blend 5% PF_3E; (■) blend 10% PF_3E

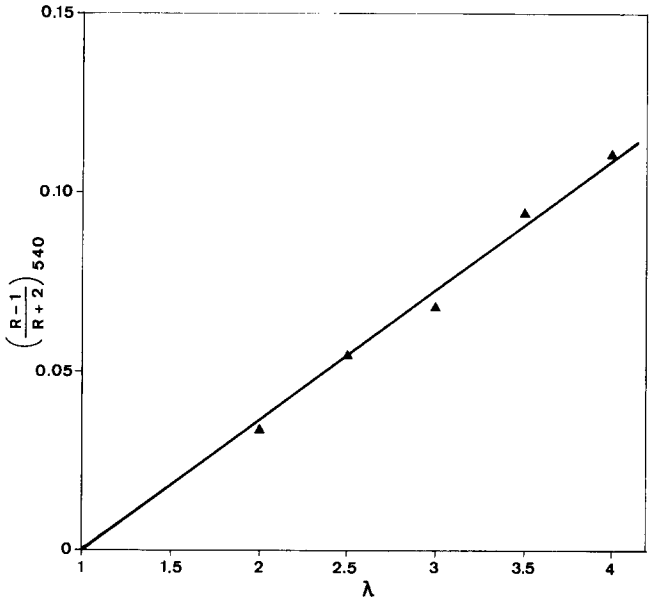

Figure 6 $(R-1)/(R+2)_{540}$ *versus* draw ratio λ for PMMA–PF_3E/1 blend containing 10% of PF_3E. Temperature of stretching $T = T_g + 23°C$. Strain rate $\dot{\varepsilon} = 0.026\ s^{-1}$

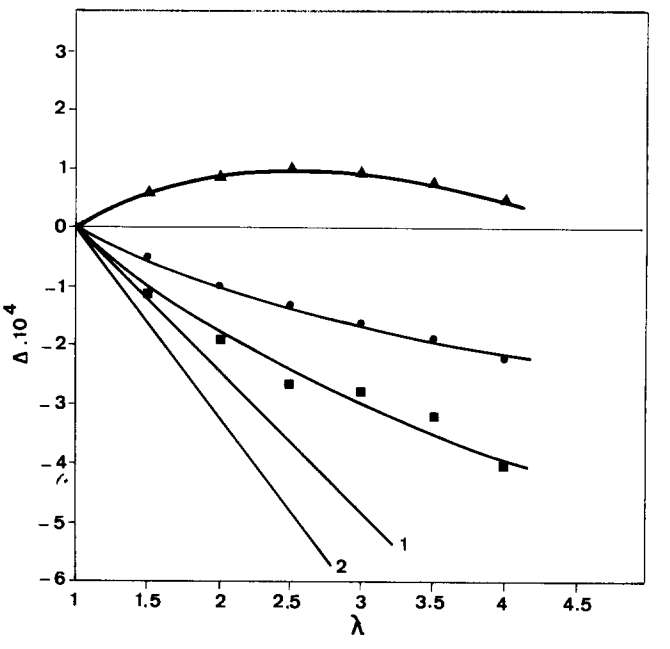

Figure 7 Birefringence Δ *versus* draw ratio λ for PMMA–PF_3E/1 homogeneous blends. Lines 1 and 2 are relative to the calculated birefringence of PMMA from infra-red data in the 5% and 10% blends, respectively. Symbols: (■) pure PMMA; (●) blend 5% PF_3E; (▲) blend 10% PF_3E

Another way to estimate PF_3E orientation is to use birefringence measurements. Although intrinsic birefringence of PF_3E is unknown, intrinsic birefringence of PMMA has been measured ($\Delta^0_{PMMA} = -50.7 \times 10^{-4}$) (ref. 20) and one can characterize PF_3E orientation by the function:

$$\langle P_2(\cos\theta)\rangle^*_{PF_3E} = \Delta^0_{PF_3E}\langle P_2(\cos\theta)\rangle_{PF_3E}$$
$$= [\Delta - f_{PMMA}\Delta^0_{PMMA}\langle P_2(\cos\theta)\rangle_{PMMA}]/(1 - f_{PMMA}) \quad (3)$$

the latter equation making use of equation (2).

Figure 7 illustrates the birefringence data obtained for different homogeneous blends stretched at $T = T_g + 23°C$ and $\dot{\varepsilon} = 0.026\ s^{-1}$. In the blends the negative birefringence of PMMA is balanced by the positive value of PF_3E birefringence. A positive birefringence results in the blend containing 10% of PF_3E/1 with a maximum value around a draw ratio between 2.5 and 3. A similar maximum value of birefringence has been previously observed in PMMA–PVF_2 blends containing 20% of PVF_2 at a draw ratio $\lambda = 2$[23].

These results show that, similarly to polystyrene–poly(2,6-dimethyl-1,4-phenylene oxide)[24] and PMMA–PVF_2[23] blends, it is possible to have oriented materials from PMMA–PF_3E blends that have good mechanical properties but no birefringence.

Figure 8 shows the change of $\langle P_2(\cos\theta)\rangle^*_{PF_3E}$ as a function of draw ratio for blends containing 5% and 10% of PF_3E/1. No significant difference is observable between the two blends. As expected, a decrease of the stretching temperature in the 5% blend results in an increase of the $\langle P_2(\cos\theta)\rangle^*_{PF_3E}$ function.

Orientation in crystallized PMMA–PF_3E blends

Besides the study of homogeneous blends, it was of interest to examine the behaviour of blends in which PF_3E has crystallized. Experiments were performed on samples containing 20% and 30% of PF_3E/2 annealed for 48 h at 160°C. As shown in *Figure 9*, thermograms of films exhibit a glass transition at 118–119°C, close to the PMMA T_g value (122°C), and a melting peak around

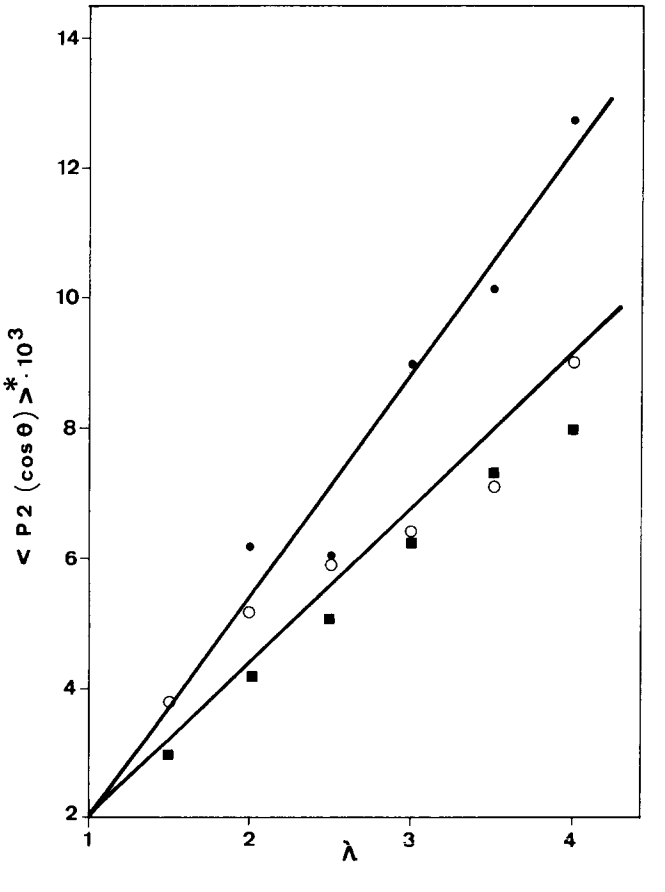

Figure 8 Orientation function $\langle P_2(\cos\theta)\rangle^*$ of PF_3E *versus* draw ratio λ for PMMA–PF_3E/1 homogeneous blends. Strain rate $\dot{\varepsilon} = 0.026\ s^{-1}$. Temperature of stretching $T = T_g + 23°C$: (■) blend 5% PF_3E; (○) blend 10% PF_3E. Temperature of stretching $T = T_g + 17°C$; (●) blend 10% PF_3E

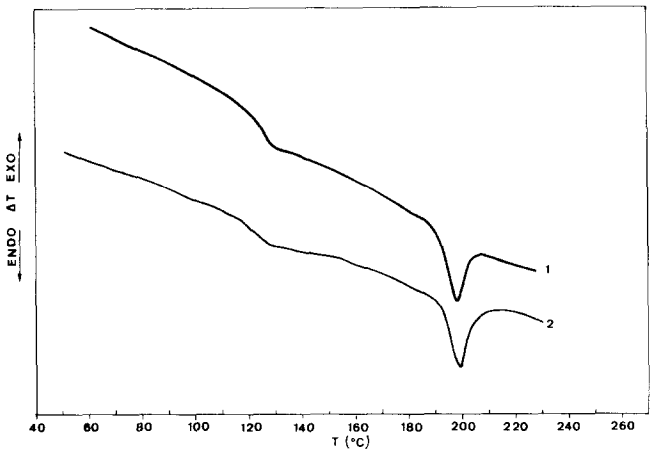

Figure 9 D.s.c. curves of crystallized PMMA–$PF_3E/2$ blends annealed 48 h at 160°C: (1) blend 20% PF_3E; (2) blend 30% PF_3E

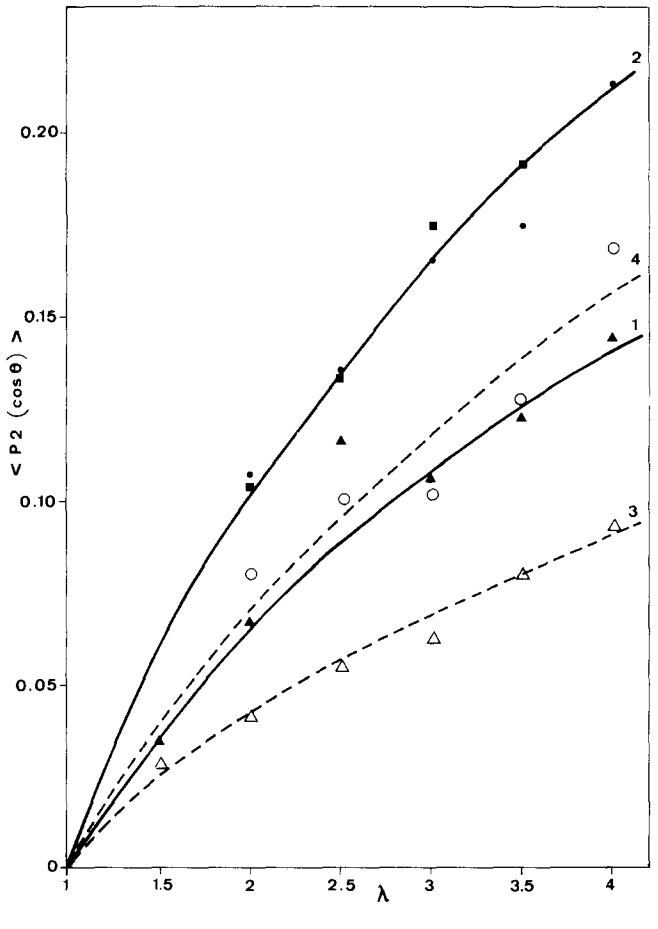

Figure 10 Orientation function of PMMA in crystallized PMMA–$PF_3E/2$ blends as a function of draw ratio. Strain rate $\dot{\varepsilon} = 0.026\ s^{-1}$. Temperature of stretching $T = T_g + 12.5°C$: (1) pure PMMA; (2) blends 20% (●) and 30% (■) PF_3E. Temperature of stretching $T = T_g + 20.5°C$: (3) pure PMMA; (4) blend 20% PF_3E

Table 2 Values of $(R-1)/(R+2)_{540}$ in oriented crystallized PMMA–$PF_3E/2$ blends at a draw ratio $\lambda = 4$ and a strain rate $\dot{\varepsilon} = 0.026\ s^{-1}$

	PF_3E (%)		
	20	20	30
Stretching temperature (°C)	131.5	139.5	131.5
$(R-1)/(R+2)_{540}$	0.60	0.58	0.68

198°C ($T_m(PF_3E) \sim 200°C$). The two blends were stretched at $T = T_g + 12.5°C$ and a strain rate $\dot{\varepsilon} = 0.026\ s^{-1}$. As shown in *Figure 10*, PMMA chain orientation is higher in the blends than in pure PMMA and remains insensitive to the amount of $PF_3E/2$. Stretching of samples containing 20% of $PF_3E/2$ at $T = T_g + 20°C$ leads to the same conclusion, the orientation obtained being, as expected, less important than the orientation achieved at $T = T_g + 12.5°C$. As a matter of fact, PF_3E crystallization induces the appearance of a PMMA phase containing about 3% of PF_3E whatever the initial PF_3E percentage in the blend. As far as PF_3E orientation is concerned, values of the function $(R-1)/(R+2)_{540}$ at a draw ratio $\lambda = 4$ are given in *Table 2*. The contribution of crystallites to orientation leads to higher values than the values obtained in homogeneous blends (see *Figure 6*). Furthermore, the stretching temperature has no influence on orientation in the 20% $PF_3E/2$ blend. This is easily understood if one considers the crystallites acting as the knots of a network with physical crosslinks. A similar effect was previously observed in a study of poly(vinyl chloride) orientational behaviour[25].

Orientation developed in the 30% $PF_3E/2$ blend is higher than the orientation achieved in the 20% $PF_3E/2$ blend. This result is well supported by an increase of crystallinity in the 30% blend. Two simultaneous phenomena must occur. On the one hand, as crystallites orient more readily than the amorphoous phase, an increase in the number and/or the degree of perfection of crystals will result in an increase of the orientation function. On the other hand, the number of physical crosslinks will increase with crystallinity and amorphous chains should also be more oriented.

CONCLUSIONS

In this study on PMMA–PF_3E blends, we have shown that one observes an increase of PMMA orientation with respect to pure PMMA in homogeneous blends stretched under the same experimental conditions ($T - T_g$ = constant), the range of concentration being up to 10% of PF_3E. On the other hand, PF_3E chain orientation is insensitive to the concentration of this polymer in the blend. An increase of stretching temperature induces a decrease of the orientation level of both polymers. The present results are in good agreement with the behaviour previously observed in other compatible blends[1,26,27], i.e. that orientation is concentration-dependent when the corresponding component is present in a large amount. The increase of orientation observed in the blends is in good agreement with an increase in the friction coefficient.

In blends in which PF_3E has crystallized, a small amount of PF_3E ($\sim$3%) remains in the PMMA amorphous phase. The orientation of this polymer is insensitive to the original PF_3E concentration and remains higher than the orientation observed in pure PMMA under the same experimental conditions. The orientation of the semicrystalline PF_3E phase increases with crystallinity but remains insensitive to the stretching temperature because of the existence of a physical network originating from the presence of crystallites.

REFERENCES

1 Zhao, Y., Jasse, B. and Monnerie, L. *Polymer* 1989, **30**, 1643

2 Noland, J. S., Hsu, N. N. C., Saxon, R. and Schmitt, J. M. *Adv. Chem. Ser.* 1971, **99**, 15
3 Nishi, T. and Wang, T. T. *Macromolecules* 1975, **8**, 909
4 Roerdink, E. and Challa, G. *Polymer* 1980, **21**, 590
5 Hoursont, O. J. and Hughes, I. D. *Polymer* 1977, **18**, 1175
6 Coleman, M. **M**., Zarian, J., Varnell, D. F. and Painter, P. C. *J. Polym. Sci., Polym. Lett. Edn.* 1977, **15**, 745
7 Wendorff, J. H. *J. Polym. Sci., Polym. Lett. Edn.* 1980, **18**, 439
8 Douglass, D. C. and McBrierty, V. J. *Macromolecules* 1978, **11**, 766
9 Lin, T. S. and Ward, T. C. *Polym. Prepr. (Am. Chem. Soc., Div. Polym. Chem.)* 1983, **24**, 136
10 Paul, D. R. and Altamirano, J. O. *Polym. Prepr. (Am. Chem. Soc., Div. Polym. Chem.)* 1974, **15**, 409
11 Yagi, T. *Polym. J.* 1979, **11**, 353
12 Tonelli, A. E., Schilling, F. C. and Cais, R. E. *Macromolecules* 1981, **14**, 560
13 Cais, R. E. and Kometani, J. M. *Macromolecules* 1984, **17**, 1933
14 Lovinger, A. J. and Cais, R. E. *Macromolecules* 1984, **17**, 1939
15 Léonard, C., Halary, J. L. and Monnerie, L. *Polymer* 1985, **26**, 1507
16 Wang, L. H. and Porter, R. S. *J. Polym. Sci., Polym. Phys. Edn.* 1874, **22**, 1645
17 Faivre, J. P., Xu, Z., Halary, J. L., Jasse, B. and Monnerie, L. *Polymer* 1987, **28**, 1881
18 Ward, I. M. 'Structure and Properties of Oriented Polymers', Applied Science, London, 1975
19 Nagai, H. *Appl. Polym. Sci.* 1963, **7**, 1697
20 Zhao, Y., Jasse, B. and Monnerie, L. *Makromol. Chem., Macromol Symp.* 1986, **5**, 87
21 Bachmann, M. A., Gordon, W. L., Koenig, J. L. and Lando, J. B. *J. Appl. Phys.* 1979, **50**, 6106
22 Kim, B. S. and Porter, R. S. *Macromolecules* 1985, **18**, 1214
23 Hahn, B. R. and Wendorff, J. H. *Polymer* 1985, **26**, 1619
24 Lefebvre, D., Jasse, B. and Monnerie, L. *Polymer* 1982, **23**, 706
25 Theodorou, M. and Jasse, B. *J. Polym. Sci. (B) Polym. Phys.* 1986, **24**, 2643
26 Faivre, J. P., Jasse, B. and Monnerie, L. *Polymer* 1985, **26**, 879
27 Bouton, C., Arrondel, V., Rey, V., Sergot, Ph., Manguin, J. L., Jasse, B. and Monnerie, L. *Polymer* 1989, **30**, 1414